Inherent Optical Properties Attenuation Coefficient Modelling for Optical Shallow Water in Kepulauan Seribu of Jakarta, Indonesia

Kuncoro Teguh Setiawan[1,2], Mohammad Syamsu Rosid[1*], Masita Dwi Mandini Manessa[3], A.A. Md. Ananda Putra Suardana[4], Novi Susetyo Adi[5], Gathot Winarso[2], Takahiro Osawa[6], Wikanti Asriningrum[2], Harsono Supardjo[1]

[1]Department of Physics, Faculty of Mathematics and Natural Sciences, Universitas Indonesia
Campus UI Depok, Jawa Barat, 16424 Indonesia
[2]Research Center for Remote Sensing, National Research and Innovation Agency
Jl. Pasir Putih Raya No.1, Ancol, Daerah Khusus Ibukota Jakarta 14430 Indonesia
[3]Department of Geography, Faculty of Mathematics and Natural Sciences, Universitas Indonesia
Campus UI Depok, Jawa Barat, 16424 Indonesia
[4]Research Center for Oceanography National Research and Innovation Agency
Jl. Pasir Putih Raya No.1, Ancol, Daerah Khusus Ibukota Jakarta 14430 Indonesia
[5]Data Center, Ministry of Marine Affairs and Fisheries Republic of Indonesia
Gedung Mina Bahari IV Lt 1. Jl. Medan Merdeka Timur No. 16 Daerah Khusus Ibukota Jakarta, Indonesia
[6]Center for Remote and Application of Satellite Remote Sensing (YUCRAS), Yamaguchi University
2-16-1 Tokiwadai, Ube 755-8611, Japan
Email: syamsu.rosid@ui.ac.id

Abstract

Technology to obtain bathymetric information has become necessary considering the length of the coastline and the many islands owned by Indonesia. Measurement technology using multi-beam and single-beam echo sounders is still an alternative to producing bathymetric information. In shallow water, using echo sounders has constraints and limitations, such as being time-consuming, costly and prone to equipment damage. Remote sensing technology is an alternative to obtaining bathymetric information in shallow waters. Bathymetric modelling with analytical and semi-analytic models from satellites requires attenuation coefficients. Therefore, attenuation coefficient models are essential for satellite data. Attenuation coefficient studies using inherent optical properties (IOP) parameters have not yet been studied to determine Kepulauan Seribu bathymetry, Jakarta, Indonesia. The IOP modelling is determined by absorption and backscatter parameters. Chlorophyll-a Total influences these parameters: Total Suspended Matter (TSM) and Coloured Dissolved Organic Matter (CDOM). This study was performed to determine the attenuation coefficient model using multispectral remote sensing in the Kepulauan Seribu and applied five approaches to determining the attenuation coefficient via IOP: the Gordon, Kirk, Morel, Lee and Simon models. The five models' IOP attenuation coefficient results were compared to the in-situ attenuation coefficient value and evaluated. The results of IOP attenuation coefficient modeling of multispectral remote sensing based on the condition of local water parameters is $K_d(\lambda) = 1.4369\ ((a(\lambda) + b(\lambda)) / \cos\theta) + 0.072$. *based on the modified Gordon method, The modelling results were obtained with an accuracy of 0.98 determination coefficient* (R^2) *and 0.029 Root Mean Square Error (RMSE).*

Keywords: *Attenuation coefficient, IOP, shallow waters, Kepulauan Seribu, Indonesia*

Introduction

Indonesia is an archipelagic country with about 17,504 islands, a coastline of 108,000 km and 77% of the ocean area of deep and shallow seas (Risnain, 2021). Technology to obtain bathymetric information has become necessary considering the length of the coastline and the many islands owned by Indonesia. Measurement technology using multi-beam and single-beam echo sounders is still an alternative to producing bathymetric information (Khomsin *et al.*, 2021; Yan *et al.*, 2018). In shallow water, using echo sounders has constraints and limitations, such as being time-consuming, costly and prone to equipment damage. Therefore, using remote sensing technology to obtain bathymetric information in shallow water is an alternative (Le *et al.*, 2022; Wan and Ma, 2021).

Remote sensing technology can use analytical and semi-analytic methods to obtain bathymetric information. Bathymetric modelling with analytical and semi-analytic models from satellites requires attenuation coefficients. Visible wavelengths are used to obtain reflections from the bottom, which are influenced by the effect of the attenuation coefficient in the water column. The interaction of visible waves

*) Corresponding author
© Ilmu Kelautan, UNDIP
https://ejournal.undip.ac.id/index.php/ijms
DOI: 10.14710/ik.ijms.29.2.222-232
Received : 11-02-2024
Accepted : 21-03-2024

in the water column weakens exponentially with depth following the Beer–Lambert law, which is caused by absorption and backscattering (Kirk, 1991; Mobley, 1994). Water depth values can be obtained using the natural logarithm of the exponential function to produce bathymetric values (Jagalingam *et al*., 2015). Unfortunately, no one has studied the attenuation coefficient using inherent optical properties (IOP) parameters to determine bathymetry, especially in the Kepulauan Seribu. This study was conducted to obtain an attenuation coefficient model in the Kepulauan Seribu, Jakarta. Therefore, attenuation coefficient modelling to obtain bathymetric information from remote sensing technology is essential (Amrari *et al*., 2021; Le Quilleuc *et al*., 2021).

Ideally, the attenuation coefficient is determined by a direct, in-field measurement via an instrument. However, the existence of instruments has problems. These tools are not only expensive but also limited in availability. Indonesia does not have a tool to measure the attenuation coefficient directly. In addition, the extent of shallow waters in Indonesia has become a problem in obtaining information on the distribution of existing attenuation coefficient values. Therefore, this model uses the IOP approach based on the radiation-energy-transfer equation. Gillis *et al*. (2020) estimate the optical properties of remote sensing reflectance measurements by combining radiation transfer models with numerical optimization. Liu *et al*. (2018) use an exponential function to show the relationship between IOP parameters and bathymetric depth from lidar measurements. Mavraeidopoulos *et al*. (2019) employed a hybrid bio-optical transformation (HBT) methodology to model IOP and AOP parameters with semi-analytical and empirical algorithms.

Studies of the attenuation coefficient were carried out in the context of modelling development by Gordon (1989), Kirk (1991), Morel and Maritorena (2001), Lee *et al*. (2002), and Simon and Shanmugam (2016). The five empirical attenuation coefficient models were established in different locations. The Gordon algorithm was developed in the Sargasso Sea, Atlantic Ocean, where seawater has visibility up to 60 m underwater. The Kirk algorithm was established in San Diego Harbor, a natural harbor in the Californian coastline's bay area with a backscatter ratio of 0.019, a value indicating low suspended solid and clear waters (Kirk, 1991). The Morel algorithm was developed in oligotrophic waters of the Pacific, where there is marine water with low surface chlorophyll-a *(Chl-a*) located in the Pacific Ocean with a value of 0.043 mg.m^{-3} (Morel and Maritorena, 2001). The Lee algorithm was developed in Baja, California, where marine waters combine between lagoons and coastal waters in Mexico and have 0.2–9.4 mg.m^{-3} *Chl-a* values (Lee *et al*., 2002). The Simon algorithm was developed in Chennai coastal waters, located in the southeastern part of India and contain *Chl-a* values ranging from 0.5–1.46 mg.m^{-3} (Simon and Shanmugam, 2016). Prasetyo *et al.* (2017) conducted research to determine the attenuation coefficient on Panggang Island, Seribu Islands, based on measuring the down-welling irradiance value ($E_d(\lambda)$). However, attenuation coefficient modelling based on IOP parameters has not been performed yet. Therefore, this research is a follow-up to determine attenuation coefficient modelling based on the abovementioned five IOP models.

All existing modelling has been carried out in water conditions different from those in the Kepulauan Seribu, which are not ocean waters and consist of many small islands. Differences in water conditions will impact the results of the attenuation coefficient model (Gomes *et al*., 2020; Zhao *et al*., 2013). The IOP attenuation coefficient modelling is determined by absorption and backscatter parameters (Bricaud *et al*., 1998). Chl-a influences these two parameters: Total Suspended Solids (*TSS*) and Coloured Dissolved Organic Matter (*CDOM*) (Morel and Maritorena, 2001; Morel *et al*., 2002). Differences in *Chl-a*, *TSS,* and *CDOM* values of a water column are influenced by several factors, including current speed, sea surface height, sea depth, sea surface temperature and coastal environmental conditions (Simon and Shanmugam, 2016). Since the values of *Chl, TSS* and *CDOM* greatly influence the algorithm results of each model, this study had to be carried out in Indonesia.

As a tropical country traversed by the equator, Indonesia is a strategic choice regarding sunlight's influence on water parameters (Val *et al*., 2005). This study aims to determine the attenuation coefficient model in the Kepulauan Seribu. Attenuation coefficient modelling results can be used to monitor the quality of shallow waters on the coast and generate shallow water bathymetric information (Mobley, 1994). The availability of bathymetric information can support economic activities of coastal resources, especially in the Kepulauan Seribu, including shipping for tourism, zoning cultivation areas and coral reef ecosystems.

Materials and Methods

The study locations in the shallow waters of Kepulauan Seribu included Putri Island, Melintang Island, Macan Island, Dolphin Island and Perak Island, at coordinate intervals of 5.570299–5.602705 south latitude and 106.537843–106.576017 east longitude (Figure 1.). Kepulauan Seribu is one of the tourist areas in Jakarta. Moreover, the area being an estuary (Irwansyah *et al*., 2023), alongside its seasonal cycle, affects water body parameters (Ahsin *et al.*, 2022; Badriana *et al.*, 2023; Kunarso *et al.*, 2023).

The study data consisted of water quality and spectral radiometer information. The field data acquired on 18–21 June 2022 consisted of temperature, salinity, conductivity, density and turbidity. The data were measured using a water checker. Meanwhile, water parameter data from laboratory analyses included *Chl-a TSS* and *CDOM*. In situ, depth data were measured using a single-beam echo sounder (Table 1).

The TriOS RAMSES spectroradiometer used to take measurements consists of three sensors. The three sensors recorded the surface remote sensing emission ($L_u(\lambda)$), sky radiance ($L_{sky}(\lambda)$) and down-welling irradiance value ($E_d(\lambda)$). Due to being near the water surface, the sensors would give a solid wave-focusing effect (Li *et al*., 2020). However, absorption and scattering of high particulate and solute content would dominate the visible light attenuation in shallow water areas (Simon and Shanmugam, 2016). The attenuation coefficient can be determined using apparent optical properties (AOP) and IOP, as the model requires both AOP and IOP parameters. Radiation transfer modelling between AOP and IOP parameters uses a radiative transfer model (RTM). An explanation of the parameters and variables used is required to understand the concept of an RTM (Table 2).

Apparent optical properties

The AOP attenuation coefficient was obtained from direct, in-field E_d measurements using the TriOS RAMSES instrument. The AOP attenuation coefficient of the down-welling recording depends on the ambient light field's geometric structure and the media's IOP, such as absorption and scattering. The availability of light as an essential regulator of phytoplankton production in the sea and on the coast is determined by the conditions of spatial, spectral, vertical and temporal changes (Simon and Shanmugam, 2013; 2016), their spectral shape for the process of classifying water types (Du *et al*., 2022; de Lucia Lobo *et al*., 2012; Simon and Shanmugam, 2016), water quality, water clarity assessment and optical bathymetry (Gholizadeh *et al*., 2016; Luis *et al*., 2019).

The attenuation coefficient (K_d), the reflectance of subsurface radiation and the reflectance of remote sensing are some parameters included in the AOP (Ambarwulan *et al*., 2013). Changes in the ambient down-welling irradiance value E_d determine the attenuation coefficient K_d. The formulation of the K_d value based on the change in the $E_d(\lambda)$ value is quantified by Equation 1 (Lee *et al*., 2002).

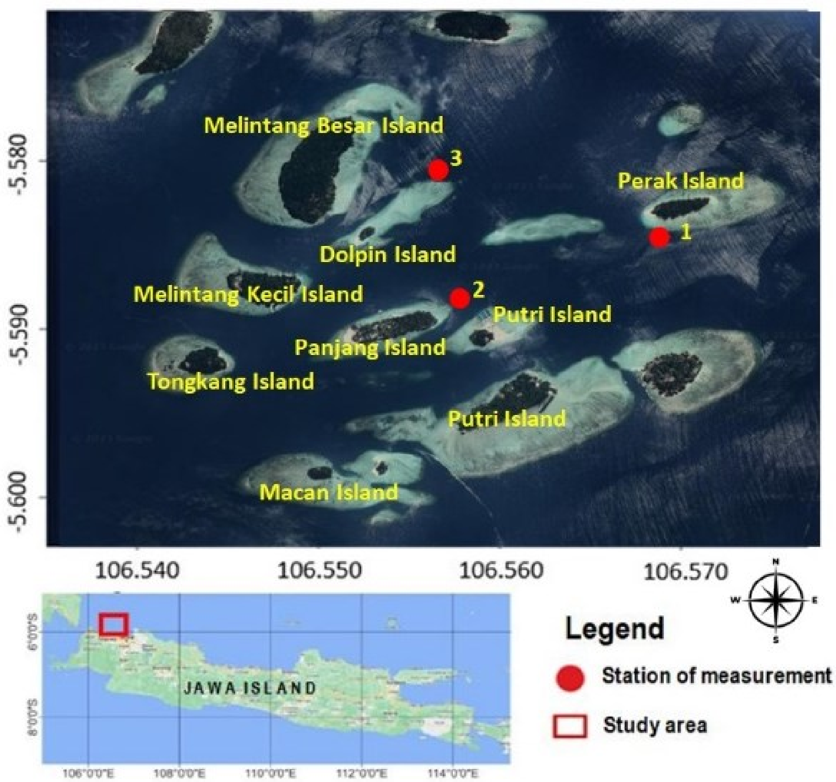

Figure 1. Study location at Seribu Islands

$$K_d(\lambda) = \frac{LnE_{d1}(\lambda) - LnE_{d2}(\lambda)}{Z_1 - Z_2} \quad \ldots 1$$

Based on Equation 1, $K_d(\lambda)$ is measured by comparing the logarithm values of the irradiance E_d at depths of Z_1 and Z_2 and the difference in depth. The $K_d(\lambda)$ AOP is the intensity attenuation of light absorbed with changes in the depth of the water through which it passes (Lee *et al*., 2002; Mobley, 1994; Simon and Shanmugam, 2016). The K_d AOP of this study was calculated by measuring the down-welling irradiance in the three stations at two different depths: 0 and 6 m.

Inherent optical Properties

The IOP model is a function of depth and optical properties in water, including absorption, backscatter and angular position of solar zenith (Simon and Shanmugam, 2016). The inverse method of modelling the down-welling-radiative diffusion attenuation coefficient to infer concentrations of dissolved and particulate constituents in shallow waters is essential for monitoring and assessing biogeochemical fluxes (Oyama *et al*., 2015; Stock, 2015; Tebbs *et al*., 2015; Simon and Shanmugam, 2016). The IOP-based attenuation coefficient models used were developed by Gordon (1989), Kirk (1991), Morel and Maritorena (2001), Lee *et al*. (2002) and Simon and Shanmugam (2016). The Gordon model is quantified by Equation 2:

$$K_d(\lambda) = 1.0935\,\frac{a(\lambda) + b_b(\lambda)}{Cos\theta} \quad \ldots 2$$

The Kirk model is quantified by Equation 3:

$$K_d(\lambda) = \frac{(a(\lambda)^2 + 0.231(a(\lambda)b_b(\lambda)))^{0.5}}{Cos\theta} \quad ..3$$

The Morel model is quantified by Equation 4:

$$K_d(\lambda) = (a_w(\lambda) + \frac{1}{2}b_w(\lambda)) + (X(\lambda)[Chl]^{e(\lambda)}) \quad ..4$$

The Lee model is quantified by Equation 5:

$$K_d(\lambda) = A + B \quad \ldots 5$$

where

$$A = (1 + 0.005\theta_s)a(\lambda)$$

$$B = 4.18(1 - 0.52e^{-10.8a(\lambda)})b_b(\lambda)$$

Finally, the Simon model is quantified by Equation 6:

$$K_d(\lambda) = \frac{1}{C_1C_2}(A_1a(\lambda) + A_2(\lambda)b_b(\lambda)a(\lambda)) + C_3) \quad .6$$

Where

$$A_1 = (1 + Cos\theta)$$

$$A_2(\lambda) = (a(\lambda)^3 + 1)$$

$$C_1 = 4.848 + 0.01696H - 4.84Cos(\theta)$$

$$C_2 = P + Q$$

$$P = 14.98 + 0.3228H - 32.312Cos(\theta)$$

$$Q = -0.3562\,HCos(\theta) + 17.65(Cos(\theta)^2)$$

$$C_3 = R + S$$

$$R = -13.13 + 0.6286H - 30.62Cos(\theta)$$

$$S = -0.1292\,H^2 - 0.2724\,HCos(\theta) + 17.14(Cos(\theta)^2)$$

The parameters of absorption (*a*) and backscatter (b_b) are determined using the IOP model approach (Bricaud *et al*., 1998; Morel and Maritorena, 2001; Morel *et al.,* 2002).

Accuracy

This modeling was verified based on the in situ AOP attenuation coefficient at three station locations (Table 1). This study commenced by determining the value of K_d based on in situ AOP down-welling irradiance measurement data. The next step focused on determining the IOP attenuation coefficient model using the Gordon, Kirk, Morel, Lee and Simon approach. Validation was done by deciding several parameters, including Pearson correlation coefficient (r_{xy}) to determine the strength of correlation between two variables, determination coefficient (R^2) to demonstrate data quality, Mean Absolute Error (*MAE*), Root Mean Square Error (*RMSE*) and Percent Error (*%Error*). The formulas of the five validation parameters of the modelling results are as follows:

$$r_{XY} = \frac{n\sum XY - \sum X \sum Y}{\sqrt{n\sum X^2 + \left(\sum X^2\right) n\sum Y^2 - \left(\sum Y\right)^2}} \quad ..7$$

$$R^2 = 1 - \frac{\sum (Y_i - X_i)^2}{\sum (Y_i - \bar{Y})^2} \quad ..8$$

$$MAE = \frac{\sum |Y_i - X_i|}{n} \quad ..9$$

$$RMSE = \left(\frac{\sum (Y_i - X_i)^2}{n}\right)^{0.5} \quad ..10$$

$$\%Error = \frac{\sum |Y_i - X_i| / Y_i}{n} \times 100\% \quad ..11$$

Note: Y = the in-situ K_d; X = K_d IOP for each model; $\bar{Y}$ = the mean in situ K_d; n = number of input data.

Table 1. Measured water quality and depth for each observation station

Station	Temp ^{0}C	Sal	Cond (mS.cm^{-1})	Density (kg.m^{-3})	Turb (FTU)	Chl (mg.m^{-3})	TSS (mg.L^{-1})	CDOM	TOM (%)	Depth (m)	Time
Station 1	30.3	32.9	55.6	1020.05	0.467	0.82	61	0.001	96.36	12.8	11:48
Station 2	30.4	32.9	55.6	1020.01	0.331	1.36	40.33	0.002	96.72	12.3	15:30
Station 3	30.5	32.9	55.7	1019.99	0.422	1.03	54.67	0.002	95.91	11.6	14:30

Table 2. Symbol and definition

Symbol (Unit)	Definition
E_d (W nm^{-1} m^{-2})	Down-welling irradiance
K_d (m^{-1})	Diffuse attenuation coefficient
a (m^{-1})	Total Absorption coefficients
a_w (m^{-1})	The absorption coefficient of pure water
a_p (m^{-1})	The absorption coefficient of phytoplankton pigments
a_y (m^{-1})	Absorption coefficient of gelbstoff
b_b (m^{-1})	Total backscattering coefficient
b_w (m^{-1})	Backscattering coefficient of pure water
b_{bp} (m^{-1})	Backscattering coefficient of suspended particles
b_p (m^{-1})	Scattering coefficient of suspended particles
Chl (mg m^{-3})	Chlorophyll-a
P (sr^{-1})	Bottom albedo
X	Coefficient
e	Coefficient
θ_s (degree)	Zenith-Sun angle
Z (m)	Water Depth

Validation was carried out by comparing the in situ K_d AOP measurement results with the K_d IOP simulation results of Gordon, Kirk, Morel, Lee and Simon models.

More details of the K_d IOP modeling research flow were created through in-situ data collection. The in-situ data measures the values of (E_d (λ)) and water quality data, including *Chl-a, TSS* and *CDOM*. Based on the E_d (λ)) value, the K_d AOP value will be determined as K_d in situ. The water quality data is converted into absorption and backscatter as IOP parameters. From the two IOP parameters, K_d IOP will be determined using five models: Gordon, Kirk, Morel, Lee, and Simon. Determination of the K_d IOP model at Kepulauan Seribu was conducted through validation and accuracy tests using regression modeling between K_d IOP on the X axis and K_d AOP on the Y axis. This methodology can show the importance of this research in advancing remote sensing methodology for the aquatic environment, especially regarding IOP and its role in interpreting K_d.

Results and Discussion

The water attenuation coefficient and down-welling irradiance that makeup water determine absorption and backscatter parameters. The water attenuation coefficient and water down-welling irradiance values were produced in the visible wavelength range because electromagnetic waves can penetrate waters (Gege and Pinnel, 2011). The E_d *(λ)* measurement results from TriOS RASMES were used to calculate the AOP attenuation coefficient. The attenuation coefficient value K_d was determined based on the blue, green and red wavelength ranges. The attenuation coefficient Kd values were determined to determine the water depth using these three wavelengths from the remote sensing images. Visible wavelengths penetrated the water column (Green *et al.*, 2000; Purkis, 2018). Data measurement in this wavelength range correlates with Lafon *et al.* (2002).

The K_d AOP value was determined based on the results of E_d measurements at two different depths. The E_d data measurements were carried out just below the water surface and at a depth of 6 m. Based on Equation 1, the attenuation coefficient K_d values were obtained at the three stations. The results of the K_d AOP calculation expressed as K_d AOP 0-6 m are shown in Table 3. At the three stations, the K_d AOP 0-6m value on the blue wave was always higher when compared to the green and red waves. This aligns with the higher blue frequency value, suggesting that the higher the wave frequency, the lower the penetration range. This condition is supported by data measurements for *Chl*, *CDOM* and

TSS (Table 1.). At Station 1, *Chl* and *CDOM* data were lower, namely 0.82 mg.m^{-3} and 0.001 (respectively), and *TSS* data were higher, namely 61 mg.L^{-1}. Table 1, shows that the three parameters *Chl*, *TSS* and *CDOM* influenced the value of K_d AOP 0-6 m. Station 1 produced the highest attenuation values, especially at blue and green wavelengths, compared to the other two stations (Figure 2.). The *Chl*, *TSS* and *CDOM* parameters were obtained from analysing water samples in the laboratory. The parameters of temperature, salinity, conductivity, density, turbidity and depth were obtained from direct, in-field measurements using a water checker.

The condition of the water quality parameters will help analyse the attenuation coefficient. Figure 2 shows the of K_d AOP 0-6 m results of the three stations. The standard deviation of the K_d results at Station 1, Station 2 and Station 3 were 0.205, 0.223 and 0.209, respectively. The standard deviation values showed the three stations' relatively similar K_d AOP 0-6 m diversity values. This condition is supported by the measurement values for the *Chl, TSS* and *CDOM* parameters in Table 1, which were not significantly different. Based on the standard deviation value, the K_d AOP 0-6 m results at Station 1 were better than the other two stations. Therefore, the K_d AOP 0-6 m at Station 1 was the K_d measurement value in the Kepulauan Seribu (Figure 3.).

Inherent optical properties

Determining the attenuation coefficient K_d using the IOP approach requires parameter values of absorption, backscatter and zenith angle. After getting the values of the absorption *(a)* and backscatter *(bb)*, the value of the IOP attenuation coefficient was determined. According to the equations of the five models, Gordon, Kirk, Lee, Morel and Simon, the attenuation coefficient was determined using the IOP approach. Equation 2 was used to determine K_d IOP using Gordon's model, Equation 3 was utilized for Kirk's model, Equation 4 was employed for Lee's model, Equation 5 was applied for Morel's model and Equation 6 was used for Simon's model. The results of the K_d calculation using the IOP approach from the five models are presented in Figure 4.

The graph of the K_d IOP results in Figure 4 shows that the Gordon, Kirk and Lee models had relatively the same values compared to the Simon and Morel models. The Morel model produced higher K_d IOP values than the Gordon, Kirk and Lee models at the three locations. This is because the Morel modelling was generated at a location in oligotrophic Pacific waters, specifically deep-sea waters with low chlorophyll values. Meanwhile, the K_d IOP value using the Simon algorithm was always low, especially at the red wavelength, but at the blue and green wavelengths, it was not too different due to the empirical Simon modelling located on the Chennai coast, which combines clear and turbid waters (Simon and Shanmugam, 2016). Therefore, from the five existing K_d IOP models, three K_d IOP models were selected to represent the K_d IOP value in the Kepulauan Seribu. This was determined based on the converging distribution of K_d IOP attenuation coefficient results for the five models in the Kepulauan Seribu. Next, verification was carried out among the three K_d IOP models with the K_d measurement results. The three K_d IOP models, namely Gordon, Kirk and Lee, were then verified and validated by comparing them to the results of K_d measurement, which were expressed as K_d from in situ measurements. Figure 5 shows the IOP attenuation coefficients based on Gordon, Kirk and Lee's models, compared with the K_d measurement.

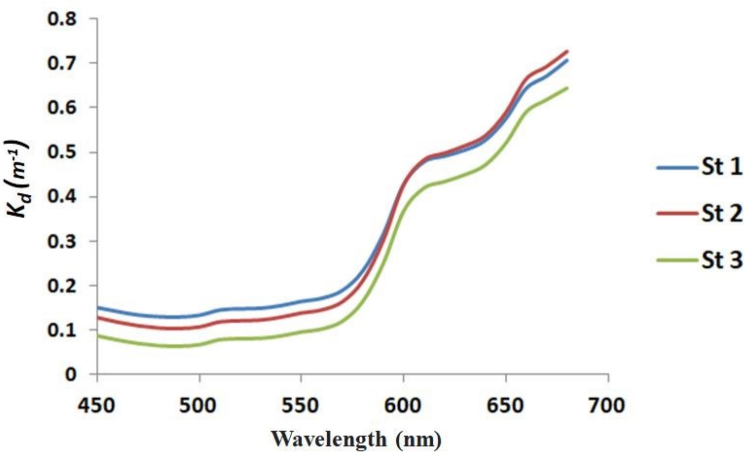

Figure 2. Plotting of K_d 0-6 m at Station 1, Station 2, Station 3

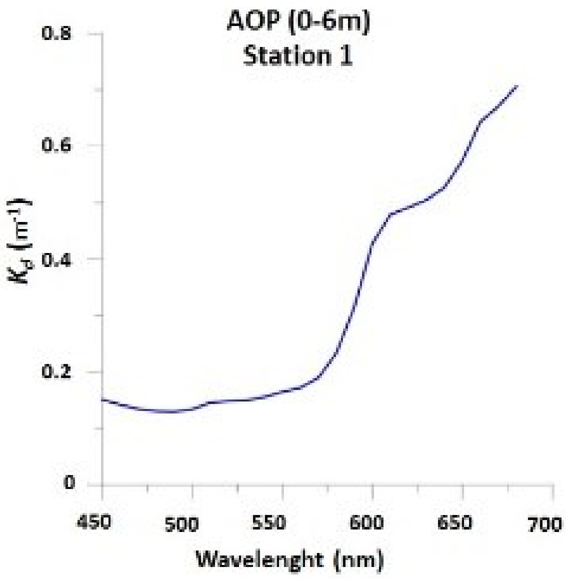

Figure 3. Plotting of K_d AOP 0-6 m at Station 1

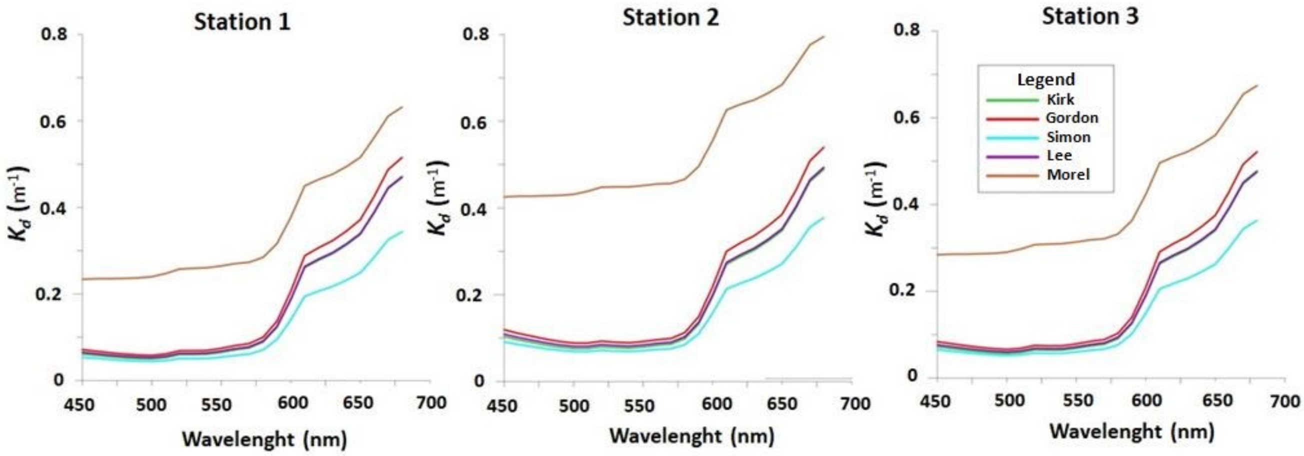

Figure 4. Comparison of the K_d from IOP models

Table 3. The results of the K_d AOP 0-6 m

K_d AOP 0-6 m	Blue (450 – 520 nm)	Green (530 – 590 nm)	Red (620 – 690 nm)
Station 1	0.13904	0.19687	0.58816
Station 2	0.11406	0.17322	0.60230
Station 3	0.07416	0.12893	0.53143

Validation was performed using several accuracy parameters to select the best IOP attenuation model from the three models. These parameters were r_{xy}, R^2, *MEA, RMSE* and *%Error*. The calculation outcomes of the five validation parameters from the three K_d IOP models with the K_d measurement results are shown in Table 4. The r_{xy} at the three stations in the models produced a value of more than 0.9. Based on these conditions, the Gordon model was the best K_d IOP model at

Kepulauan Seribu, with an r_{xy} value of 0.989, an R^2 of 0.98, an *MEA* of 0.129 and an *RMSE* of 0.141.

Gordon's K_d IOP attenuation coefficient model was the robust algorithm despite still giving an error value. The error value was modelled for the K_d IOP of the waters at Kepulauan Seribu, which have local-specific absorption and backscatter parameter values. Based on these results, further modifications were made to Gordon's K_d IOP model to produce a specific K_d IOP model in the Kepulauan Seribu. Furthermore, the K_d IOP modelling in the Kepulauan Seribu was carried out. The Kepulauan Seribu K_d IOP was built using the Gordon (best model) model. The modelling began by comparing the results of Gordon's K_d IOP with the K_d measurements. The comparison of the Gordon model's K_d IOP values and K_d measurement can be seen in Figure 6. Linear regression modelling was created using a data pair of Gordon's K_d IOP and K_d measurement to produce K_d IOP at Kepulauan Seribu. The result of K_d IOP attenuation coefficient modelling in the Kepulauan Seribu is shown in Figure 7. Based on the linear regression modelling, the resulting K_d IOP Kepulauan Seribu equation is as follows:

$$K_d(\lambda) = 1.4369\,\frac{a(\lambda) + b_b(\lambda)}{Cos\theta} + 0.072 \qquad ..12$$

Kepulauan Seribu's IOP model produces a coefficient of 1.4369 compared to the Gordon model, and a constant of 0.072 is added. This equation is influenced by the conditions of absorption and backscatter parameters in the Kepulauan Seribu and in the Sargasso Sea, Atlantic Ocean. These two parameters describe the adaptation of attenuation modeling in the Sargasso Sea, Atlantic Ocean, to the Kepulauan Seribu. This condition shows that the attenuation coefficient in the Kepulauan Seribu is close to 1.5 times that in the Sargasso Sea, Atlantic Ocean. The K_d IOP Kepulauan Seribu model results were validated based on the accuracy parameters of r_{xy}, R^2, *MEA, RMSE* and *%Error*, accounting for 0.989, 0.98, 0.022, 0.029 and 8.66%, respectively. The distribution graph of Kepulauan Seribu K_d IOP and K_d AOP is shown in Figure 7.

This method has limitations because measuring in situ data and lacking theoretical understanding may affect the attenuation prediction results for interpreting ocean colur data (Padial and Thomaz, 2008; Gomes *et al.*, 2018). This condition causes dependence on obtaining K_d (490) data from the marine colour satellite sensor using semi-analytical algorithms (Jamet *et al.*, 2010; Huang and Yao, 2017). Although this method is less accurate in predicting attenuation in cloudy, shallow waters due to absorption by *CDOM* and phytoplankton and backscattering by suspended sediments, it tends to increase attenuation in the water column (Kvale and Meissner, 2017).

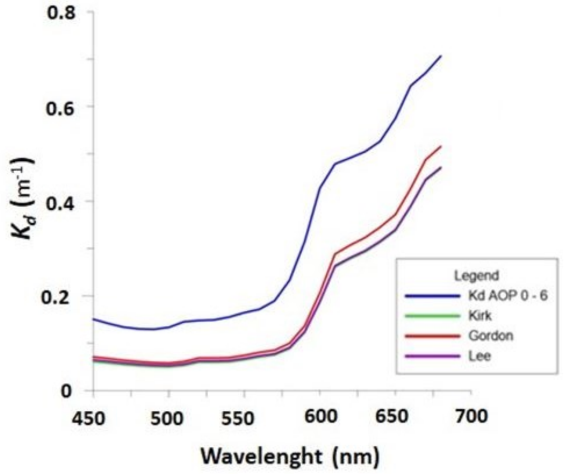

Figure 5. Comparison of K_d AOP 0-6 m and K_d IOP models

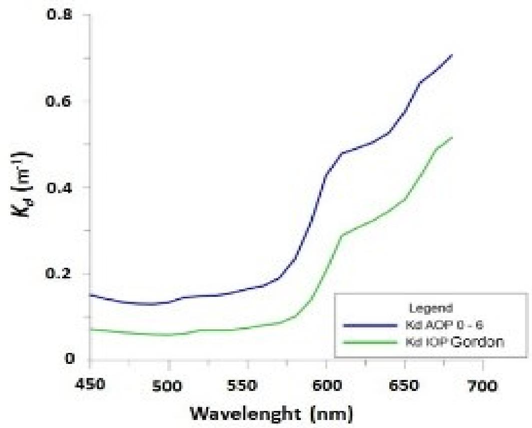

Figure 6. Plotting of K_d AOP 0-6 m and K_d IOP Gordon

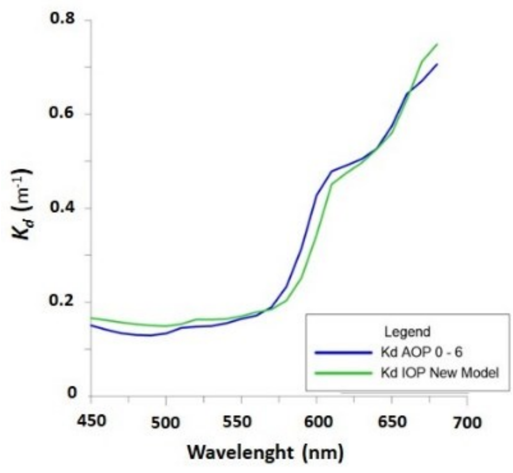

Figure 7. Plotting of K_d AOP and K_d IOP Kepulauan Seribu

Table 4. Accuracy assessment

Model K_d	Person Correlation	R^2	MEA	RMSE	% Error
Gordon	0.989	0.98	0.129	0.141	47.56
Kirk	0.989	0.98	0.149	0.163	53.60
Lee	0.989	0.98	0.146	0.160	52.04

Conclusion

Five Attenuation coefficient studies (Gordon, Kirk, Lee, Morel, and Simon's) using IOP attenuation coefficient models were applied in the shallow waters in the Kepulauan Serib. As a result, Gordon's approach(1989) showed the best IOP attenuation coefficient model in Kepulauan Seribu based on the accuracy parameters The result of modified Gordon modelling for the specific attenuation coefficient at Kepulauan Seribu is $K_d(\lambda) = 1.4369\ ((a(\lambda) + b(\lambda)) / \cos\theta) + 0.072$. The modelling result was obtained with an accuracy level of $R^2 = 0.98$ and $RMSE = 0.029$.

Acknowledgment

This study is supported by the RISPRO 2020 Program with grant number PRJ-41/LPDP/2020, in collaboration between the Geography Department Universitas Indonesia with the Ministry of Research Technology and Higher Education and Remote Sensing Research Center, BRIN.

References

Ahsin, A., Hartati, R., Widianingsih, Sitorus, E. D., Azizah, H. & Endrawati, H. 2022. Oceanographic Factors on Coastal Aggregation of Reef Manta (*Mobula alfredi*) in The Manta Sandy, Raja Ampat, Indonesia. *Ilmu Kelautan: Indonesian Journal of Marine Science*, 27(4): 330–340. https://doi.org/10.14710/ik.ijms.27.4.330-34 0

Ambarwulan, W., Widiatmaka & Budhiman, S. 2013. Deriving Inherent Optical Properties from Meris Imagery and In Situ Measurment using Quasi-analytival Algorithm. *Int. J. Remote Sens. Earth Sci.*, 10(1): 1–8. http://dx.doi.org/10.30536/j.ijreses.2013.v10.a1835

Amrari, S., Bourassin, E., Andréfouët, S., Soulard, B., Lemonnier, H. & Le Gendre, R. 2021. Shallow water bathymetry retrieval using a band-optimization iterative approach: Application to new caledonia coral reef lagoons using sentinel-2 data. *Remote Sens.*, 13(20): 4108. https://doi.org/10.3390/rs13204108

Badriana, M.R., Nur, A.A., Hidayatullah, A.I., Prastyo, A.W., Bernawis, L.I., Jeon, C., Radjawane, I.M. & Park, H. 2023. Seasonal Monitoring of Ocean Parameter Over Green Mussel Cultivation area in West Part of Cirebon Seawater. *Ilmu Kelautan: Indonesian Journal of Marine Science*, 28(1): 69–80. https://doi.org/10.14710/ik.ijms.28.1.69-80

Bricaud, A., Morel, A., Babin, M., Allali, K. & Claustre, H. 1998. Variations of light absorption by suspended particles with chlorophyll a concentration in oceanic (case 1) waters: Analysis and implications for bio-optical models. *J. Geophys. Res. Oceans, 103*(C13): 31033–31044. https://doi.org/10.1029/98JC02712

de Lucia Lobo, F., de Moraes Novo, E.M.L., Barbosa, C.C.F. & Galvão, L.S. 2012. Reference spectra to classify Amazon water types. *Int. J. Remote Sens.*, 33(11): 3422–3442. https://doi.org/10.1080/01431161.2011.627391

Du, Y., Song, K. & Liu, G. 2022. Monitoring Optical Variability in Complex Inland Waters Using Satellite Remote Sensing Data. *Remote Sens.*, 14(8): 1–17. https://doi.org/10.3390/rs14081910

Gege, P. & Pinnel, N. 2011. Sources of variance of downwelling irradiance in water. *Appl. Opt.*, 50(15): 2192–2203. https://doi.org/10.1364/AO.50.002192

Gholizadeh, M.H., Melesse, A.M. & Reddi, L. 2016. A comprehensive review on water quality parameters estimation using remote sensing techniques. *Sensors*, 16(8): p.1289. https://doi.org/10.3390/s16081298

Gillis, D.B., Bowles, J.H., Montes, M.J. & Miller, W.D. 2020. Deriving bathymetry and water properties from hyperspectral imagery by spectral matching using a full radiative transfer model. *Remote Sens. Lett.*, 11(10): 903–912. https://doi.org/10.1080/2150704X.2020.1795293

Gomes, A.C.C., Bernardo, N., Carmo, A.C.D., Rodrigues, T. & Alcântara, E. 2018. Diffuse attenuation coefficient retrieval in CDOM dominated inland water with high chlorophyll-a concentrations. *Remote Sens.*, 10(7): 1063. https://doi.org/10.3390/rs10071063

Gomes, A.C., Alcântara, E., Rodrigues, T. & Bernardo, N. 2020. Satellite estimates of euphotic zone and Secchi disk depths in a colored dissolved organic matter-dominated inland water. *Ecol. Indic.*, 110: 105848. https://doi.org/10.1016/j.ecolind.2019.105848

Gordon, H.R. 1989. Can the Lambert-Beer law be applied to the diffuse attenuation coefficient of ocean water?. *Limnol. Oceanogr.*, 34(8): 1389–1409. https://doi.org/10.4319/lo.1989.34.8.1389

Green, E.P., Mumby, P.J., Edwards, A.J. & Clark, C.D. 2000. Remote Sensing Handbook for Tropical Coastal Management. France: Coastal Management Sourcebooks 3, p.316.

Huang, C. & Yao, L. 2017. Semi-analytical retrieval of the diffuse attenuation coefficient in large and shallow lakes from GOCI, a high temporal-resolution satellite. *Remote Sens.*, 9(8): p.825. https://doi.org/10.3390/rs9080825

Irwansyah, Isma, F., Ismida, Y., Isma, M.F., Sufahani, S.F. & Akbar, H. 2023. Effect of Stream River and Tidal on the Suspended Sediment Concentration of Kuala Langsa Estuary, Aceh, Indonesia. *Ilmu Kelautan: Indonesian Journal of Marine Science*, 28(1): 27–36. https://doi.org/10.14710/ ik.ijms.28.1.27-36

Jagalingam, P., Akshaya, B.J. & Hegde, A.V. 2015. Bathymetry mapping using landsat 8 satellite imagery. *Procedia Eng.*, 116: 560–566. https://doi.org/10.1016/j.proeng.2015.08.326

Jamet, C., Loisel, H. & Dessailly, D. 2010. Empirical nonlinear determination of the diffuse attenuation coefficient Kd(490) in coastal waters from ocean color images. *Remote Sens. Coast. Ocean, Land, Atmos. Environ.*, 7858: 54-59. https://doi.org/10.1117/12.869730

Khomsin, Pratomo, D. G. & Saputro, I. 2021. Comparative analysis of singlebeam and multibeam echosounder bathymetric data. *IOP Conf. Ser. Mater. Sci. Eng.*, 1052(1): 012015. https://doi.org/10.1088/1757-899x/1052/1/012015

Kirk, J.T.O. 1991. Volume scattering function, average cosines, and the underwater light field. *Limnol. Oceanogr.*, 36(3): 455–467. https://doi.org/10.4319/lo.1991.36.3.0455

Kunarso, Ismunarti, D.H., Rifa'i, A., Munandar, B., Wirasatriya, A. & Susanto, R.D. 2023. Effect of Extreme ENSO and IOD on the Variability of Chlorophyll-a and Sea Surface Temperature in the North and South of Central Java Province. *Ilmu Kelautan: Indonesian Journal of Marine Science*, 28(1): 1–11. https://doi.org/10.14710/ik.ijms.28.1.1-11

Kvale, K.F. & Meissner, K.J. 2017. Primary production sensitivity to phytoplankton light attenuation parameter increases with transient forcing. *Biogeosciences*, 14(20): 4767–4780. https://doi.org/10.5194/bg-14-4767-2017

Lafon, V., Froidefond, J.M., Lahet, F. & Castaing, P. 2002. SPOT shallow water bathymetry of a moderately turbid tidal inlet based on field measurements. *Remote Sens. Environ.*, 81(1): 136–148. https://doi.org/10.1016/S0034-4257(01)00340-6

Le Quilleuc, A., Collin, A., Jasinski, M. F. & Devillers, R. 2021. Very high-resolution satellite-derived bathymetry and habitat mapping using pleiades-1 and icesat-2. *Remote Sens.*, 14(1): p.133. https://doi.org/10.3390/rs14010133

Le, Y., Hu, M., Chen, Y., Yan, Q., Zhang, D., Li, S., Zhang, X. & Wang, L. 2022. Investigating the Shallow-Water Bathymetric Capability of Zhuhai-1 Spaceborne Hyperspectral Images Based on ICESat-2 Data and Empirical Approaches: A Case Study in the South China Sea. *Remote Sens.*, 14(14): p.3406. https://doi.org/10.3390/rs14143406

Lee, Z., Carder, K.L. & Arnone, R.A. 2002. Deriving inherent optical properties from water color: a multiband quasi-analytical algorithm for optically deep waters. *Appl. Opt.*, 41(27): 5755-5772. https://doi.org/10.1364/ao.41.005755

Li, C.Y., Shih, R.S. & Weng, W.K. 2020. Investigation of ocean-wave-focusing characteristics induced by a submerged crescent-shaped plate for long-crested waves. *Water*, 12(2): p.509. https://doi.org/10.3390/w12020509

Liu, Q., Liu, D., Bai, J., Zhang, Y., Zhou, Y., Xu, P., Liu, Z., Chen, S., Che, H., Wu, L., Shen, Y. & Liu, C. 2018. Relationship between the effective attenuation coefficient of spaceborne lidar signal and the IOPs of seawater. *Opt. Express*, 26(23): 30278-30291. https://doi.org/10.1364/OE.26.030278

Luis, K.M.A., Rheuban, J.E., Kavanaugh, M.T., Glover, D.M., Wei, J., Lee, Z. & Doney, S.C. 2019. Capturing coastal water clarity variability with Landsat 8. *Mar. Pollut. Bull.*, 145: 96–104. https://doi.org/10.1016/j.marpolbul.2019.04.078

Mavraeidopoulos, A.K., Oikonomou, E., Palikaris, A. & Poulos, S. 2019. A hybrid bio-optical transformation for satellite bathymetry modeling using Sentinel-2 imagery. *Remote Sens.*, 11(23): p.2746. https://doi.org/10.3390/rs11232746

Mobley, C. 1994. Optical Properties of Water. Light and waters: Radiative Transfer in Natural Waters. Academic Press. 592p.

Morel, A. & Maritorena, S. 2001. Bio-optical properties of oceanic waters: A reappraisal. *J. Geophys. Res.*, 106(C4): 7163–7180. https://doi.org/10.1029/2000JC000319

Morel, A., Antoine, D. & Gentili, B. 2002. Bidirectional reflectance of oceanic waters: accounting for Raman emission and varying particle scattering phase function. *Appl. Opt.*, 41(30): 6289–6306. https://doi.org/10.1364/ao.41.006289

Oyama, Y., Fukushima, T., Matsushita, B., Matsuzaki, H., Kamiya, K. & Kobinata, H. 2015. Monitoring levels of cyanobacterial blooms using the visual cyanobacteria index (VCI) and floating algae index (FAI). *Int. J. Appl. Earth Obs. Geoinf.*, 38: 335–348. https://doi.org/10.1016/j.jag.2015.02.002

Padial, A.A. & Thomaz, S.M. 2008. Prediction of the light attenuation coefficient through the Secchi disk depth: Empirical modeling in two large Neotropical ecosystems. *Limnol.*, 9: 143–151. https://doi.org/10.1007/s10201-008-0246-4

Prasetyo, B.A., Siregar, V.P., Agus, S.B. & Asriningrum, W. 2017. In-Situ Measurement of Diffuse Attenuation Coefficient and Its Relationship With Water Constituent and Depth Estimation of Shallow Waters By Remote Sensing Technique. *Int. J. Remote Sens. Earth Sci.,*14(1): 47-60. https://doi.org/10.30536/j.ijreses.2017.v14.a2682

Purkis, S.J. 2018. Remote sensing coral reefs. *Encyclopedia of Ocean Sciences* (3rd ed.). Elsevier Inc. https://doi.org/10.1016/B978-0-12-409548-9.10813-9

Risnain, M. 2021. the Concept of the Archipelagic Province and Archipelagic State in the Perspective of National and International Law. *Lampung J. Int. Law*, *3*(2): 73–84. https://doi.org/10.25041/lajil.v3i2.2367

Simon, A. & Shanmugam, P. 2013. A new model for the vertical spectral diffuse attenuation coefficient of downwelling irradiance in turbid coastal waters: validation with in situ measurements. *Opt. Express*, 21(24): 30082-30106. https://doi.org/10.1364/oe.21.0300 82

Simon, A. & Shanmugam, P. 2016. Estimation of the spectral diffuse attenuation coefficient of downwelling irradiance in inland and coastal waters from hyperspectral remote sensing data: Validation with experimental data. *Int. J. Appl. Earth Obs. Geoinf.*, 49: 117–125. https://doi.org/10.1016/j.jag.2016.02.003

Stock, A. 2015. Satellite mapping of Baltic Sea Secchi depth with multiple regression models. *Int. J. Appl. Earth Obs. Geoinf.*, 40: 55–64. https://doi.org/10.1016/j.jag.2015.04.002

Tebbs, E.J., Remedios, J.J., Avery, S.T., Rowland, C.S. & Harper, D.M. 2015. Regional assessment of lake ecological states using Landsat: A classification scheme for alkaline-saline, flamingo lakes in the East African Rift Valley. *Int. J. Appl. Earth Obs. Geoinf.*, 40: 100–108. https://doi.org/10.1016/j.jag.2015.03.010

Val, A.L., De Almeida-Val, V.M.F. & Randall, D.J. 2005. Tropical Environment. *Fish Physiol.*, 21: 1–45. https://doi.org/10.1016/S1546-5098(05)21001-4

Wan, J. & Ma, Y. 2021. Shallow Water Bathymetry Mapping of Xinji Island Based on Multispectral Satellite Image using Deep Learning. *J. Indian Soc. Remote Sens.*, 49(9): 2019–2032. https://doi.org/10.1007/s12524-020-01255-9

Yan, Z.L., Qin, L.L., Wang, R., Li, J., Wang, X.M., Tang, X.L. & An, R.D. 2018. The application of a multi-beam echo-sounder in the analysis of the sedimentation situation of a large reservoir after an Earthquake. *Water,* 10(5): p.557. https://doi.org/10.3390/w10050557

Zhao, J., Barnes, B., Melo, N., English, D., Lapointe, B., Muller-Karger, F., Schaeffer, B. & Hu, C. 2013. Assessment of satellite-derived diffuse attenuation coefficients and euphotic depths in south Florida coastal waters. *Remote Sens. Environ.*, 131: 38–50. https://doi.org/10.1016/j.rse.2012.12.009